Role of GLP1-receptor-mediated α-β-cell communication in functional β-cell heterogeneity.

Nirmala V. Balasenthilkumaran[#1], Lidija Križančić Bombek[#2], David Ramirez[1], Maša Skelin Klemen[2], Eva Paradiž Leitgeb[2], Jasmina Kerčmar[2], Jan Kopecky[2], Yaowen Zhang[1], Maria Skjott Hansen[3], Yidi Shao[4], Annanya Sethiya[1], Adam Takaoglu[1], Divya Prabhu[1], Aining Fan[1], Shravani Vitalapuram[1], Christian M. Cohrs[5,6,7], Stephan Speier[5,6,7], Jurij Dolenšek[2], Marko Gosak [2,8,9], Richard K.P. Benninger*[3], Andraž Stožer*[2], Vira Kravets*[1,10].

[#]equal contributions, *corresponding authors.

[1] Department of Bioengineering, Jacobs School of Engineering, University of California San Diego, San Diego, CA, United States of America.

[2] Institute of Physiology, Faculty of Medicine, University of Maribor, Maribor, Slovenia.

[3] Department of Bioengineering, Barbara Davis Center for Diabetes, Aurora, Colorado, United States of America, Barbara Davis Center for Childhood Diabetes, University of Colorado Anschutz Medical Campus, Aurora, Colorado, United States of America.

[4] Department of Electrical and Computer Engineering, Jacobs School of Engineering, University of California San Diego, San Diego, CA, United States of America.

[5] Institute of Physiology, Medical Faculty Carl Gustav Carus, Technical University of Dresden, Dresden, Germany.

[6] Paul Langerhans Institute Dresden of the Helmholtz Zentrum München at the University Clinic Carl Gustav Carus of Technische Universität Dresden, Helmholtz Zentrum München, Neuherberg, Germany

[7] German Center for Diabetes Research (DZD), München-Neuherberg, Germany

[8] Faculty of Natural Sciences and Mathematics, University of Maribor, Maribor, Slovenia

[9] Alma Mater University, Maribor, Slovenia

[10] Department of Pediatrics, School of Medicine, University of California San Diego, San Diego, CA, United States of America.

Email ID: vkravets@ucsd.edu, Telephone no: +1 (858) 246-3567

Word Count: 3970, Figure count: 5

Key Words

GLP1-R, α-β communication, β-cell heterogeneity, diabetes, 1st responder, hub cell.

Abstract

While islet β-cells were first viewed as a singular functional entity, since the 1970s findings reveal that individual β-cells differ in their insulin secretion. More recently distinct functional subpopulations based on differential calcium dynamics have been demonstrated to drive islet function. Here, we investigate how paracrine signaling, specifically glucagon-like peptide receptor (GLP-1R)-mediated α-β-cell communication shapes functional β-cell heterogeneity. To address this, we utilized confocal imaging of calcium responses in isolated islets from GCaMP6s mice and in islets from pancreatic slices of C57BL/6 mice, both before and after a GLP-1R antagonist (exendin-9) treatment. Inhibiting α-β-cell communication prolonged response time, increased 1st phase heterogeneity, and decreased the 1st phase response peak. Additionally, it reduced 2nd phase oscillation frequency and heterogeneity, thereby enhancing 2nd phase coordination across β-cells. These changes were more pronounced in α-neighboring β-cells. Moreover, addition of exendin-9 disrupted the temporal consistency and α-cell proximity of hub-cells and (to a lesser degree) 1st responder β-cells. Together, these findings underscore the importance of engineering islets containing both α- and β-cells for stem cell-derived islet replacement therapies for Type-1diabetes.

Article Highlights

- Role of GLP-1R mediated α–β cell communication in functional β-cell heterogeneity was unclear.
- Does GLP-1R inhibition affect all β-cells uniformly, or will α-neighboring cells be affected more? Is existence of 1st responder and hub cell subpopulations shaped by GLP-1R signaling?
- GLP-1R inhibition decreases multiple metrics or β-cell responsiveness - especially in α-neighboring β-cells. It diminishes spatiotemporal consistency of hub β-cells and (to a lesser degree) 1st responders.
- Islet-local GLP-1R communication in absence of exogenous GLP-1 is sufficient for significant control of β-cell function. Incorporating α-cells into the engineered islets can improve islet replacement outcomes.

Introduction

Diabetes mellitus is an endocrine disease characterized by high blood glucose levels, primarily resulting from decreased insulin secretion or from insulin resistance. The insulin-producing β-cells exhibit different transcriptomic profiles, protein expression, and gap junction coupling (1-5). These variations result in a heterogeneous response to glucose stimulation, leading to the existence of distinct subpopulations of β-cells within the islet. We and others have previously shown the existence, temporal and spatial stability of unique functional β-cell subpopulations within the islet (6-8). Recent studies have attempted to identify markers that could separate β-cell subpopulations. PSA-NCAM-expressing and Fltp-Venus positive β-cells have been shown to exhibit enhanced insulin secretion and improved overall cell function (5; 9; 10). However, these markers are not always linked to β-cell functionality, leaving the mechanisms shaping these β-cell subpopulations poorly understood (9).

Islets of Langerhans also contain glucagon-secreting α-cells and somatostatin-secreting δ-cells, which interact through paracrine signaling (11; 12). Glucagon secreted by α-cells is sensed by glucagon and GLP-1 receptors (Gcg-R, GLP-1R) on β-cells, enhancing glucose-stimulated cyclic AMP, calcium ([Ca^{2+}]) influx, and insulin secretion (13; 14). The β-cells located closer to α- and δ- cells are likely to be more strongly influenced, contributing to greater heterogeneity in their responses (11; 15-17). We have previously shown that immune cells preferentially interact with α-cell-rich regions of an islet in pre-T1D, which combined with previous reports of higher levels of HLA-1 and IL-1β expression in α-cells during early T1D illustrate importance of α-cells both in health and diabetes (18-20). Understanding the extent to which α-cells influence β-cell function and heterogeneity in healthy conditions aids better understanding of diabetes pathophysiology.

During glycolysis, β-cells generate intracellular ATP, which binds to and closes ATP-sensitive potassium channels, causing membrane depolarization. This depolarization triggers the opening of voltage-gated calcium channels, leading to an increase in intracellular [Ca^{2+}] and subsequent insulin release. The insulin release, therefore, correlates with the [Ca^{2+}] response, and they both are biphasic with a well-defined transitional 1st phase followed by an oscillatory 2nd phase (21-24). β-cells are electrically excitable and their electrical activity propagates from one cell to another across the islet via connexin36 (cx36) gap junctions, resulting in a coordinated response to glucose stimulation (25; 26). The 1st phase of an islet's response can be characterized by its peak amplitude and time of response to glucose (6). The oscillatory 2nd phase can be characterized by oscillation frequency, active time, or time lag (27). Finally, the coordination of response can be quantified by functional networks, where β-cell pairs within an islet are linked based on the coordination of [Ca^{2+}] dynamics (7; 28). The extent to which these parameters of β-cell function are influenced by α-cells remains unclear.

Here, we investigate the GLP-1R-mediated role of α-cells in β-cell's 1st and 2nd phase response to glucose, and in shaping of the functional β-cell subpopulations.

Research Design and Methods

Ethics Statement: Protocols for islet isolation from mice with β-cell–specific GCaMP6s expression were approved by the University of Colorado Institutional Animal Care and Use Committee (IACUC Protocol number: 00024). Protocols for pancreatic slices from C57BL/6J mice were in accordance with the European and national legislation and approved by the Administration for Food Safety, Veterinary Sector and Plant Protection of the Republic of Slovenia (permit numbers U34401-35/2018-2). Islet isolation and pancreatic slices were carried out using previously published protocols (6; 29).

Fixing and post-staining of islets: After functional imaging, islets were fixed with 4% PFA, permeabilized with 0.25% Triton X-100 in blocking buffer and blocked with 5% BSA in PBS. Islets were incubated with antibodies for 1 day and imaged the following day. Isolated islets were stained with anti-insulin (eBioscience, 53-9769-82; 1:100 dilution) and anti-glucagon (Bioss, bs-3796R-Cy5; 1:100 dilution) antibodies. Islets from slices were stained with anti-insulin (eBioscience, 53-9769-82; 1:100 dilution), anti-glucagon (eBioscience, 41-9743-82; 1:10 dilution), and anti-somatostatin (eBioscience, 50-9751-82; 1:40 dilution) antibodies.

Glucose stimulation protocol and [Ca^{2+}] imaging: One hour prior to imaging, the islets or slices were incubated in an imaging solution containing BMHH and BSA or HBS (for slices) and 2mM glucose. [Ca^{2+}] imaging was performed at 37°C with a 10 min baseline at 2mM glucose, followed by 20 min stimulation at 11mM. Glucose was then lowered to 2mM for 20 min before a second 20 min 11 mM glucose stimulation. In the experimental group, 100nM ex-9 (Sigma Aldrich, E7269) was added during the 2nd part of the protocol (beginning at the second low glucose incubation).

Isolated islets were imaged using either an LSM780 system (Carl Zeiss, Oberkochen, Germany) with a 40×1.2 NA objective or an LSM800 system (Carl Zeiss) with a 20×0.8 NA Plan-Apochromat objective, using a 488 nm laser to excite the GCaMP6s fluorescence. Time-series was recorded 10–15 µm from the islet surface at 1 Hz and 256×256 resolution. Pancreatic slices were imaged using either a Leica TCS SP5 AOBS Tandem II upright confocal system with a 20×1.0 NA HCX APOL water immersion objective, or a Leica TCS SP5 DMI6000 CS inverted confocal system with a 20×0.7 NA HC PL APO water/oil immersion objective, with a 488 nm laser used to excite the [Ca^{2+}]-sensitive dye. Time-series were collected 15 µm from the islet surface at 2 Hz and 512×512 resolution.

Analysis of [Ca^{2+}] dynamics: Cells were manually segmented from their [Ca^{2+}] time series using ImageJ (FIJI) (30). Custom MATLAB routines were used to perform single-cell analysis of [Ca^{2+}] dynamics. *1st phase analysis*: The peak height was defined as the most prominent local maximum during the 1st phase response to glucose. Response time (T_{resp}) was defined as the time at which the [Ca^{2+}] intensity reached 50% of the peak. T_{resp} of 20 minutes was assigned for cells that were unresponsive in either of the two stimulations. *2nd phase frequency analysis*: Consistent window sizes were analyzed across both stimulations, beginning just prior to the 1st oscillation of the 2nd phase. A low-pass filter of 0.03 Hz was applied to isolate the slow frequency component, which was subtracted from the raw data to obtain a 'residual' time course. This residual was detrended and smoothed using a 4th-order Butterworth filter. A high-pass filter (cutoff: 1 Hz) was subsequently applied, and peaks were identified as regions where the signal exceeded the threshold: mean(residual) + 2×σ(residual) (31). The time between consecutive peaks was measured to calculate the oscillation frequency. *2nd phase network analysis*: A band-pass filter (0.02 and 0.5 Hz) was first applied, followed by smoothing with a moving average filter (window size 2) (32). Pairwise Pearson correlation coefficients were then computed to generate a correlation matrix based on the temporal similarity between [Ca^{2+}] traces (28; 33). In the 1st glucose stimulation, two cells were linked if their correlation exceeded a pre-set correlation threshold adjusted in each islet to yield an average of approximately eight connections per cell (34). In the 2nd stimulation, this threshold determined from the 1st stimulation was applied. The average number of links per cell in the 2nd stimulation (K_{avg}) was calculated by dividing the total number of links by the number of cells.

α-cell neighborhood: We first applied background subtraction and median filtering using ImageJ to process the immunofluorescence (IF) images. We then overlaid and aligned the IF images with the [Ca^{2+}] time series. Spheres of diameter 25 μm and centered in the individual

β-cells were constructed. For each β-cell, the local α-cell neighborhood was calculated by quantifying the percent of glucagon-positive volume contained within the corresponding sphere, normalized to the volume of the sphere.

First responder domain analysis: β-cells in different islets were categorized into different domains, based on their 1st phase response-time. Each cell in a domain responded after the local 1st responder. See supplemental information for more details.

Statistical analysis: All statistical analysis was performed using GraphPad Prism (GraphPad, Boston, United States of America). Data are presented as box plots with min/max whiskers or paired scatter plots. Box plots illustrate the distribution of individual values (median ± IQR) with the mean indicated by a '+', while paired scatter plots connect data points from the same islet across different conditions. Exact p-values are reported, and differences were considered statistically significant for $p < 0.05$.

Results

Spatial location of the 1st responders. The 1st responders were identified as a functional subpopulation of β-cells that drive the islet's 1st phase [Ca^{2+}] response to high glucose stimulations (6). We recorded [Ca^{2+}] dynamics in the live islets and then fixed and post-stained these islets for insulin and glucagon (**Fig. 1A and 2A**). We also utilized the pancreatic slice model, as the enzymatic digestion during islet isolation may affect the number of α-cells on the islet periphery. The pancreatic slice platform offers the advantage of the unperturbed α-cell numbers on the islet periphery, while also possessing the disadvantage of dissection of an islet during slicing.

The 1st responders were located closer to the islet periphery than to the core in isolated islets (**Fig. 1B**) and in islets from slices (**Fig. 2B**). Since in mouse islets, α-cells are mostly located at the islet periphery, we indeed observed that 1st responders have significantly higher number of α-cell neighbors compared to the last responders in both isolated islets and in islets from slices ($p = 0.0431$ and 0.0411) (**Fig. 1C** and **2C**).

GLP-1R signaling potentiates islet-average 1st phase of response to glucose. As depicted in **Fig. 1D** and **2D**, and in Methods section, islets were consecutively stimulated with glucose (control group). In the experimental group, α-β-cell communication was inhibited by the addition of 100 nM ex-9 during the 2nd low glucose incubation and 2nd glucose stimulation. On average, in the 2nd glucose stimulation the response time, T_{resp}, was shorter for the control group and longer for the ex-9 treated isolated islets and islets in slices ($p < 0.0001$; **Fig. 1E** and **2E**). Additionally, we found a greater decrease ($p = 0.0001$ and $p < 0.0001$) in the 1st phase peak amplitude in ex-9 treated islets, compared to the control group in both models (**Fig. 1F** and **2F**). This reflects the role of GLP-1R signaling in enhancing and accelerating the 1st phase [Ca^{2+}] response.

GLP-1R signaling has a mild effect on the spatial location of 1st responders. On ex-9 addition, we observed a decrease in the percentage of the 1st responders that were part of the same 1st responder cluster (same-cell, 1st or 2nd nearest neighbors) in the 1st stimulation. Significant effect was observed in isolated islets ($p = 0.0497$) and, to a lesser extent (trend present but not significant), in pancreatic slices ($p=0.2346$) (**Fig. 1G** and **2G**). Additionally, 1st responders in islets from slices were identified significantly closer ($p < 0.0001$) to the islet core upon ex-9 addition (**Fig. 2H**). In contrast, their spatial distribution remained largely unchanged in control islets and in experiments with isolated islets (**Fig. 1H** and **2H**). Furthermore, we

observed a significant decrease in the α-cell proximity of 1st responders in the slices (p=0.0080) (**Fig. 2I**). This trend was present but not significant in isolated islets (p = 0.3859) (**Fig. 1I**). Hence, α-cells do play a role in maintaining the spatiotemporal consistency of 1st responders, albeit to a various extent in isolated islets vs in pancreatic slice model.

GLP-1R signaling coordinates the 1st phase β-cell response to glucose. In isolated islets, we first plotted the distribution of T_{resp} of all the β-cells in each islet, centered around the median T_{resp} (**Fig. 3A**). To assess the spread of T_{resp} within an islet, we then plotted the variance of T_{resp} distribution in the 1st vs 2nd stimulations (**Fig. 3B**). We observed a higher T_{resp} variance upon ex-9 addition (**Fig. 3B, 3C**), consistent with our previous findings (35). **Fig. 3C** summarizes the data presented in **Fig. 3B**, showing that the increase in heterogeneity of T_{resp} in ex-9 stimulations was significantly different than in control stimulations (p = 0.0259), illustrating that inhibition of GLP-1R mediated α-β-cell communication enhances the heterogeneity of β-cell response.

GLP-1R communication increases the speed of [Ca^{2+}] signal propagation in the 1st phase. We next tested whether ex-9-induced increase in T_{resp} heterogeneity could be attributed to weaker [Ca^{2+}] signal generated by the 1st responders. Since β-cell responses often occur within localized clusters or domains (36), we created an automated, bias-free '1st responder domain' recognition algorithm as shown in **Fig. 3D** and **Supplementary Fig. S1**. Each domain consists of a local 1st responder initiating the [Ca^{2+}] signal propagating to all the other β-cells in the domain. Within each domain, the slope of the distance between each β-cell to the local 1st responder vs β-cell's response time indicated the speed of the [Ca^{2+}] signal for that domain (see **Fig. 3E**). In every islet, the speed of signal propagation was normalized to the mean speed across all domains in the 1st stimulation. The speed of signal propagation decreased

significantly upon ex-9 addition ($p < 0.0001$) (**Fig. 3F**). We observed no changes ($p = 0.2228$ and $p = 0.4572$) in domain size in both control and ex-9 treated islets (see Fig. 3G).

Number of α-cells positively correlates with frequency of [Ca^{2+}] oscillations in β-cells. We quantified the frequency of [Ca^{2+}] oscillations during the 2nd phase [Ca^{2+}] response to glucose and identified the islet cell types based on IF (**Fig. 4A**). In most islets with a higher α-cell count, we observed a higher oscillatory frequency (**Fig. 4B**), aligning with previously published findings (37). To test whether GLP-1R signaling in the islet influences the oscillatory [Ca^{2+}] response of β-cells, we applied ex-9 as before (**Fig. 4C**). We calculated the signal to noise ratio (SNR) of each cell's [Ca^{2+}] trace (see Methods). We observed a significant decrease ($p < 0.0001$) in frequency after ex-9 treatment (**Fig. 4D**), whereas control islets exhibited a frequency increase.

We next assessed heterogeneity in frequency responses in individual β-cells by calculating the width of frequency distribution in the 1st vs 2nd stimulation for each islet (**Fig. 4E**). We observed a trend towards a narrower frequency distribution upon ex-9 addition ($p = 0.0625$), and no changes in control islets (**Fig. 4F**).

Proximity to α-cells affects the magnitude of the β-cell's response to ex-9: To test if the β-cells near α-cells are influenced more than those without α-cell neighbors, we aligned the [Ca^{2+}] time series recordings with their corresponding IF images (**Fig. 4G** and **4I**) and computed the α-cell neighborhood for each β-cell. The β-cells with α-cell neighborhood greater than zero were termed "α-neighboring" and β-cells with zero α-cell neighborhood as "non α-neighboring". Notably, we observed a significantly greater increase in frequency ($p < 0.0001$) in α-neighboring β-cells in control experiments (**Fig. 4H**). On ex-9 treatment, α-neighboring β-cells exhibited a significantly greater ($p = 0.0014$) decrease in frequency (**Fig. 4J**). These

findings suggest that α-cells exert localized influence on β-cell frequency of [Ca^{2+}] oscillations during the 2nd phase of the response.

Steady-state 2nd phase functional connectivity is increased under GLP-1R inhibition. To assess coordination of [Ca^{2+}] responses, we generated functional β-cell networks for the 1st and 2nd stimulations (**Fig. 5A, B)**. We observed a significant increase in connectivity in ex-9-treated islets during the 2nd stimulation ($p < 0.0001$, **Fig. 5C**). We hypothesize that this was due to the GLP-1R inhibition exerting a homogenizing effect on oscillation frequency across the islet (described in **Fig. 4F**). A narrower frequency distribution leads to a higher coordination of [Ca^{2+}] activity.

GLP-1R inhibition leads to lower number of hub-cells in the α-cell-rich neighborhoods. Hub-cells were identified as functional β-cell subpopulation that coordinate β-cell [Ca^{2+}] oscillations in the islet (7). As previously defined, we considered hub-cells to be the β-cells with greater than 60% of the node degree distribution (38). We quantified α-cell neighborhood in the immediate proximity of each hub cell in 1st vs 2nd stimulations (**Fig. 5D**). In control islets, there was no difference, whereas in ex-9–treated islets hub cells were found significantly less frequently in α-cell-rich neighborhoods ($p=0.0404$, **Fig. 5F**). Since there were two possible reasons for the observed change, *i.e.,* significant change in connectivity of (1) α-neighboring cells or (2) of the non- α-neighboring β-cells, we tested which of these two mechanisms was at play. In both control and ex-9 conditions α-neighboring β-cells exhibited almost no change in connectivity (bars with yellow borders **Fig. 5E, F**) compared to significant changes in connectivity of non-α-neighboring β-cells (bars with grey borders **Fig. 5E, F**). Finally, addition of ex-9 disrupted spatial consistency of hub cells overall ($p = 0.0687$; **Fig. 5G**).

Together with results illustrated in **Fig.4**, these findings suggest that GLP-1R-mediated α-β communication is supporting hub-cell phenotype in the distance-dependent manner with respect to α-cells. At the same time, this effect enhances heterogeneity in [Ca^{2+}] oscillation frequency across the islet diminishing overall connectivity in control conditions, while this effect is reversed by addition of ex-9.

Discussion

In previous α-β-cell communication studies, different islets were used for control and the experimental group, introducing inter-islet variability. In our study, the 1st stimulation (glucose only) served as a baseline for the 2nd stimulation in the same islet (glucose only - control, or glucose with ex-9 – experimental group). This allowed us to rule out the effects of islet heterogeneity. In previous studies, the manipulation of α–β signaling was achieved by the absence of glucagon and GLP-1 receptors (13; 14; 39), or addition of exogenous glucagon. In contrast, we pharmacologically inhibited α-β cell communication within the *same islet* using ex-9. This approach, while technically more complex, allowed us direct comparison of changes in the abundance of functional subpopulations and α–cell proximity of the 1st responder and hub cells upon GLP-1R inhibition. We demonstrated that the 1st phase strength and speed as well as the 2nd phase oscillation frequency and functional connectivity, are all significantly affected when β-cells do not utilize their GLP-1R, and most importantly, that these effects are more predominant in α-neighboring β-cells.

Why do α-cells accelerate the timing of β-cell's response to high glucose?

Glucagon binds to the GLP-1 and glucagon receptors in the β-cells (13; 14; 40; 41). However, recent studies show that α-β- glucagon signaling is primarily achieved via the GLP-1R, as Gcg-R knockout mice exhibit normoglycemia (40-42). When glucagon binds the GLP-1R, it

interacts with the Gαs subunit, which subsequently activates adenylyl cyclase, resulting in cAMP production (43). cAMP activates both the protein kinase A (PKA) and Epac2A signaling pathways, amplifying insulin secretion (44). PKA phosphorylates key exocytotic proteins, facilitating [Ca^{2+}] release and insulin granule exocytosis, while also targeting the Kir6.2 subunit in the K_{ATP} channels to promote K_{ATP} channel closure and membrane depolarization (45-47). Consequently, the observed acceleration of the 1st phase [Ca^{2+}] response could be attributed to increased activity of L-type voltage-dependent [Ca^{2+}] channels (VDCCs), which increase voltage-dependent [Ca^{2+}] currents. The inhibition of these channels was shown to reduce [Ca^{2+}] response (48; 49). When [Ca^{2+}] enters the islet through VDCCs, the resultant increase in cytoplasmic [Ca^{2+}] triggers additional [Ca^{2+}] release from the endoplasmic reticulum, via [Ca^{2+}]-induced-[Ca^{2+}] release (CICR), which has previously been shown to be also facilitated by exendin 4, a GLP-1 agonist (50; 51). Inhibition of Epac2A and PKA diminishes exendin-4-induced CICR, while their activation restores it, suggesting a potential mechanism through which GLP-1R signaling may amplify [Ca^{2+}] dynamics and insulin secretion (52). Consistent with these findings, exendin-4 has been shown to enhance β-cell activation and [Ca^{2+}] responses (53).

Hence, we speculate that due to increased cAMP concentrations in the presence of glucagon, β-cells respond more readily to glucose stimulation, resulting in a faster and amplified response. In the presence of a GLP-1R antagonist such as ex-9, there is a significant decrease in cAMP production, and therefore β-cells are less ready to respond to glucose stimulations, resulting in a decreased [Ca^{2+}] response in the 1st phase (54).

How do α-cells decrease heterogeneity of β-cell response in the 1st phase?

The 1st phase [Ca^{2+}] response has previously been shown to originate in β-cells with elevated excitability (6). Time delays in activation among β-cells reflect electrical coupling, with [Ca^{2+}]

waves propagating across the islet (55). Here we demonstrated that GLP-1R mediated paracrine signaling mildly accelerates the T_{resp} of the islet and enables the β-cells closer to α-cells to respond faster to glucose stimulations (see Fig. **1C**, **1E**, **2C** and **2E**). Additionally, we observed an increase in β-cell heterogeneity upon blocking α-β cell communication (see **Fig. 3B** and **3C**). We also observed a decrease in the amplitude of 1st phase [Ca^{2+}] response (see **Fig. 1F** and **2F**) on ex-9 treatment, which likely reflects a decrease in the strength of [Ca^{2+}] signal generated by β-cells. This diminished signal strength is increasing heterogeneity in T_{resp}. While gap junction coupling is another factor that could influence the speed of [Ca^{2+}] wave propagation (25), β-cell activity was recorded only 20 mins after ex-9 treatment, a timescale insufficient to induce significant changes in Cx36 expression and gap junction coupling.

Why do α-cells increase the frequency of β-cell [Ca^{2+}] oscillations?

An overall increase in oscillation frequency has previously been reported following the addition of cAMP agonists (56; 57). GLP-1 and glucagon have also been shown to induce cAMP oscillations, which leads to an increase in [Ca^{2+}] oscillations (43; 58). Moreover, cAMP oscillations in β-cells have been found to synchronize with [Ca^{2+}] activity and modulate both PKA and Epac2A signaling (43; 59). Interestingly, in our study the change in oscillation frequency upon ex-9 addition (see **Fig. 4D**) was more pronounced in α-neighboring β-cells (see Fig. **4H** and **4J**). We suggest that the paracrine effects of glucagon signaling are likely stronger in α-neighboring β-cells due to diffusion of α-cell secretion products, resulting in more pronounced frequency changes upon GLP-1R inhibition. As discussed in the previous section, ex-9 treatment may reduce cAMP oscillations, thereby contributing to the observed decrease in 2nd phase [Ca^{2+}] oscillations (54).

How does α-β communication impact different functional β-cell subpopulations?

We identified that 1st responders are primarily located at the islet periphery with a higher α-cell neighborhood in their immediate vicinity compared to last responders (see **Fig. 1B**, **1C**, **2B** and **2C**). Previously, ~67% of 1st responders were found to contain a readily releasable insulin granule pool, exhibit higher vitamin B6 production, and lower K_{ATP} conductance, supporting the idea of cell-autonomous, intrinsic properties of this subpopulation (6; 60; 61). Ex-9 moderately reduced the spatiotemporal consistency and α-cell proximity of 1st responders, suggesting a non-cell-autonomous contribution from α-cells in stability of this functional subpopulation (see **Fig. 1G**, **2G, 1I** and **2I**). However, spatial location of the 1st responders was relatively unchanged on ex-9 addition in the isolated islet model and the decrease in α-cell neighborhood also remained statistically non-significant (see **Fig. 1H** and **1I**). Therefore, while 1st responder phenotype is stabilized by GLP-1R-mediated communication, it is not an essential parameter of this population's existence.

Hub cells, have been shown to display increased gap junctional conductance and metabolism through elevated glucokinase expression, with recent studies emphasizing the importance of metabolic coupling and intrinsic properties in defining hub identity (7; 38). Ex-9 reduces cAMP levels, an effect likely more pronounced in β-cells neighboring α-cells, which normally experience elevated cAMP due to glucagon signaling (43; 54). cAMP activates PKA, which phosphorylates key components of the electron transport chain, thereby enhancing ATP production, oxidative phosphorylation, and overall metabolic activity (62). Here we reported a decrease in the temporal consistency of hub cells and α-cell proximity upon ex-9 treatment (see **Fig. 5E-G**), likely due to a decline in glucose metabolism in α-neighboring β-cells. Based on these findings, we conclude that GLP-1R-mediated α–β signaling is important for the cellular metabolism and maintaining hub cell phenotype.

Conclusions

Overall, our study emphasizes the importance of GLP-1 receptor and α–β-cell communication in supporting β-cell function and maintenance of β-cell subpopulations. Several studies have shown how the loss of these specialized functional subpopulations leads to a disproportionate decline in overall islet β-cell performance. Since α-β-cell communication was found to elicit faster β-cell responses, higher 1st phase peak amplitudes, and increased 2nd phase oscillation frequency, designing islets that include both α- and β-cells may offer a more effective strategy for stem-cell-derived islet replacement therapies in the treatment of T1D.

Acknowledgements

We thank Dr. Marko Sterk of the University of Maribor, Slovenia for their involvement in developing the network analysis algorithm.

Author Contributions

N.B. performed data analysis and wrote the manuscript; L.K.B. prepared tissue slices, collected experimental data, edited manuscript; D.R. wrote analysis code and performed data analysis; M.S.K., E.P.L., J.K., J.K., M.S.H. collected experimental data, Y.Z., Y.S., A.S., A.T., D.P., A.F., S.V. performed data analysis, C.M.C. and J.D. aided in experimental design, data collection, and edited manuscript; S.S., M.G., R.K.P.B., A.S. aided in the study design and edited the text, V.K. designed the study, wrote analysis code, collected and analyzed data, edited text.

Funding Information

Work was supported by Burroughs Wellcome Fund CASI Award number G-1021870.01 or 1220467 (to VK), NIH-NIDDK HIRN "Emerging leaders in type 1 diabetes" grant number HIRN, RRID:SCR_014393; UC24 DK104162 (to VK), Institute of Physiology Faculty of Medicine at the Technische Universität Dresden, by the Paul Langerhans Institute Dresden (PLID) of the Helmholtz Zentrum München at the University Clinic Carl Gustav Carus of Technische Universität Dresden, and the German Ministry for Education and Research to the German Centre for Diabetes Research (to CMC and SS), Slovenian Research Agency (research core funding nos. P3-0396 and I0-0029, as well as research projects nos. J3-60062 and L3-60156) (to MG, JD, AS), U34401-12/2018/2, Slovenian Research and Innovation Agency (to LKB). R01 DK106412 (to RKPB); R01 DK102950 (to RKPB); and the University of Colorado Diabetes Research Center (DRC) P30 DK116073 (to RKPB).

Online Supplemental Materials

All experimental data and MATLAB analysis routines will be made publicly available through an online data repository following acceptance for publication.

Figure Captions

Figure 1. Effect of ex-9 and α-cell proximity on the β-cell 1st phase [Ca^{2+}] response to glucose in isolated islets. (A) Representative live islet with β-cell-specific GCaMP6s [Ca^{2+}] indicator used to record time series, all cells visualized via backscatter, and nuclei visualized

via Hoechst; IF z-stack after this islet was fixed; live and fixed image overlay based on the backscatter signal. **(B)** Comparison of the location of 1st and last responders in the islet relative to the center of the islet (n = 20 islets). Value 1 corresponds to the islet surface, 0 – to the islet core (center of the optical 2D plane). **(C)** Comparison of α-cell neighborhood in the immediate proximity of 1st and last responders in the 1st glucose stimulation (n = 6 islets). **(D)** Experimental protocol and representative [Ca^{2+}] time course of an ex-9-treated GCaMP6s isolated islet, along with representative islet snapshots at different time points. **(E)** Time of response to glucose of each β-cell in 1st vs 2nd stimulations. Orange - in control and purple - ex-9 treated islets. Change of response time quantified as differences in response time (2nd – 1st stimulations). Negative values indicate faster responses in the 2nd stimulation, and positive values indicate slower responses (n = 11 control and n = 11 ex-9 treated islets). **(F)** 1st phase peak amplitude of each β-cell in 1st vs 2nd stimulations. Orange - control and purple - ex-9 treated islets. Change of peak height quantified as differences in peak heights (2nd – 1st stimulations). Negative value corresponds to decrease of the peak height in 2nd stimulation (n = 9 control, and n = 9 ex-9-treated islets). **(G)** Consistency of 1st responders: percent of the cells identified as a 1st responder in the 2nd stimulation that were also a 1st responder, 1st nearest neighbor, or 2nd nearest neighbor (same cell cluster) in the 1st stimulation (n = 19 control and n = 11 ex-9-treated islets). **(H)** Location of 1st and last responders relative to the center of the islet in the 1st and 2nd stimulations (n = 11 control and n = 11 ex-9 treated islets). **(I)** Comparison of α-cell neighborhood in the immediate proximity of 1st responders in the 1st and 2nd stimulations (n = 2 control and n = 4 ex-9 treated islets). Experiments were performed in isolated islets for all the data presented in this figure. Wilcoxon matched-pairs signed-rank test was used for statistical analysis in the first two graphs in panels **(E)** and **(F)**, whereas Mann-Whitney test was used for all other graphs. Outliers were removed using the ROUT method (Q = 1%).

Figure 2. Effect of ex-9 and α-cell proximity on the 1st phase β-cell [Ca^{2+}] response to glucose in islets from pancreatic slices. (A) Representative live islet stained with a [Ca^{2+}] indicator (Calbryte) used to record time series; IF z-stack after this islet was fixed; live and fixed image overlay based on the [Ca^{2+}] signal. **(B)** Comparison of the location of 1st and last responders in the islet relative to the center of the islet (n = 13 islets). Value 1 corresponds to the islet surface, 0 – to the center of the optical 2D plane. **(C)** Comparison of α-cell neighborhood in the immediate proximity of 1st and last responders in the 1st glucose stimulation (n = 9 islets). **(D)** Experimental protocol and representative [Ca^{2+}] time course of an ex-9-treated islet from a pancreatic slice stained with a [Ca^{2+}] indicator, along with representative islet snapshots at different time points. **(E)** Time of response to glucose of each β-cell in 1st vs 2nd stimulations. Orange - in control and purple - ex-9 treated islets. Change of response time quantified as differences in response time (2nd – 1st stimulations). Negative values indicate faster responses in the 2nd stimulation, and positive values indicate slower responses (n = 8 control and n = 6 ex-9 treated islets). **(F)** 1st phase peak amplitude of each β-cell in 1st vs 2nd stimulations. Orange - control and purple - ex-9 treated islets. Change of peak height quantified as differences in peak heights (2nd – 1st stimulations). Negative value corresponds to decrease of the peak height in 2nd stimulation (n = 6 control, and n = 5 ex-9-treated islets). **(G)** Consistency of 1st responders: percent of the cells identified as a 1st responder in the 2nd stimulation that were also a 1st responder, 1st nearest neighbor, or 2nd nearest neighbor (same cell cluster) in the 1st stimulation. Control and ex-9-treated islets were compared (n = 9 control and n = 6 ex-9-treated islets). **(H)** Location of 1st and last responders relative to the center of the islet in the 1st and 2nd stimulations in control and ex-9 treated islets (n = 8 control and n = 5 ex-9 treated islets). **(I)** Comparison of α-cell neighborhood in the immediate proximity of 1st responders in the 1st and 2nd stimulations in control and ex-9-treated islets (n = 5 control and n = 4 ex-9 treated islets). Experiments were performed in islets from

pancreatic slices for all the data presented in this figure. Wilcoxon matched-pairs signed-rank test was used for statistical analysis in the first two graphs in panels **(E)** and **(F)**, whereas Mann-Whitney test was used for all other graphs. Outliers were removed using the ROUT method (Q = 1%).

Figure 3. Effect of GLP-1R mediated α-β- cell communication on heterogeneity and speed of excitation propagation in β-cell during the 1st phase [Ca^{2+}] response to glucose. (A) Visualization of heterogeneity of 1st phase response time of individual cells in the islets (red represents the islet with the highest variance, and blue represents the islet with the least variance in response time). For each group, the mean and standard deviation were used to generate and plot a Gaussian curve (shown here). **(B)** Width of the response time distribution for 1st vs 2nd stimulations (n = 8 control and n = 11 ex-9 treated islets; Wilcoxon matched-pairs signed-rank test was used for statistical analysis). **(C)** Difference in the width of response-time distributions of 1st vs 2nd stimulations: comparison between control and ex-9 treated islets (n = 8 control and n = 11 ex-9 treated islets). **(D)** Pseudo-colored islet cells, based on their time of response to glucose and response time 'domains' each with the local 1st responder. Domain boundaries were identified based on the linear dependence of the response time vs distance to the local 1st responder (like shown in **(E)**). **(F)** Speed of [Ca^{2+}] signal propagation (normalized to each islet's mean domain speed during the 1st stimulation): comparison between 1st and 2nd stimulations in control and ex-9 treated islets (n = 10 control and n = 10 ex-9 treated islets). **(G)** Domain area (normalized to each islet's mean domain area during the 1st stimulation): comparison between 1st and 2nd stimulations in control and ex-9 treated islets (n = 4 control and n = 4 ex-9 treated islets). All experiments in this figure were performed in isolated islets. Mann-Whitney test was used for statistical analysis in **(C)** - **(G)**. Outliers were removed using the ROUT method (Q = 1%).

Figure 4. Effect of GLP-1R mediated α-β- cell communication on frequency of [Ca^{2+}] oscillations in β-cell during the 2nd phase response to glucose. (A) A representative islet with immunofluorescence staining for insulin, glucagon, somatostatin and a 3D segmentation of α- and δ- cells done in Imaris from the IF image. **(B)** Relationship between the islet-average frequency of [Ca^{2+}] oscillations and number of α-cells in the islet (n = 12 islets, n = 5 from isolated islets and n = 7 from pancreatic slices; Simple linear regression was used for statistical analysis). **(C)** Representative [Ca^{2+}] traces and the time windows (in purple) used for frequency and functional network analysis in the 1st and 2nd stimulations. **(D)** Change in oscillation frequency between 1st vs 2nd stimulations: comparison between control vs ex-9 treated islets (n = 9 control and n = 5 ex-9 treated islets). **(E)** Frequency distribution in individual cells in the islets (red represents the islet with the highest variance, and blue represents the islet with the least variance in frequency). For each group, the mean and standard deviation were used to generate and plot a Gaussian curve (shown here). **(F)** Islet-average frequency distribution width in 1st vs 2nd stimulations. Orange - in control vs purple – in ex-9 treated islets. Differences in frequency (2nd minus 1st stimulation) are shown in the third graph of the panel (F) (n = 8 control and n = 5 ex-9 treated islets). **(G)** Control: Time-projection of [Ca^{2}] time series; heatmap representing change in oscillation frequency between two stimulations; z-projection of the IF image with α-cells segmented in Imaris in a representative islet within a slice. **(H)** Change in oscillation frequencies in 1st vs 2nd stimulation in control islets (n = 6 islets): comparison between α-neighboring vs non α-neighboring β-cells. **(I)** Same as (G), but for ex-9 treated islet **(J)** Same as in (H) but in ex-9 treated islets (n = 4 islets). Experiments were performed in islets from pancreatic slices for all the data presented in this figure (except panel (B)). Only cells with var(signal) > 0.25σ(noise) were utilized for frequency analysis of the data presented in this figure. Mann-Whitney test was used for statistical analysis in (D), (F), (H), Outliers were removed using the ROUT method (Q = 1%).

Figure 5. Effect of GLP-1R mediated α-β-cell communication on functional connectivity in islets from pancreatic slices. (A) Functional networks in the 1st and 2nd stimulations for a representative control islet and **(B)** for a representative ex-9 treated islet. **(C)** Change in the average number of functional links (k_{avg}) in 1st vs 2nd stimulation: comparison between control vs ex-9 (n = 8 control and n = 4 ex-9 treated islets). **(D)** α-cell neighborhood in the immediate proximity of hub-cells in the 1st vs 2nd stimulations. Orange - in control and purple - in ex-9-treated islets (n = 5 control and n= 3 ex-9 treated islets). **(E)** Control: Connectivity of [Ca^{2+}] dynamics in 1st vs 2nd stimulations: comparison between α-neighboring (yellow border) and non α-neighboring β-cells (grey border). Last panel of (E) shows a change in connectivity between (2nd – 1st stimulations) for α-neighboring vs non α-neighboring β-cells (n = 5 islets). **(F)** Same as (E), but for ex-9. **(G)** Consistency of hub cells: percent of the cells identified as a hub in the 2nd stimulation that were also a hub, 1st nearest neighbor, or 2nd nearest neighbor (same cell cluster) in the 1st stimulation. Control and ex-9-treated islets were compared (n = 8 control and n = 4 ex-9-treated islets). Experiments were performed in islets from pancreatic slices for all the data presented in this figure. Wilcoxon matched-pairs signed-rank test was used for statistical analysis in the first two graphs in panels **(E)** and **(F)**, whereas Mann-Whitney test was used for all other graphs. Outliers were removed using the ROUT method (Q = 1%).

References

1. Benninger RKP, Kravets V: The physiological role of β-cell heterogeneity in pancreatic islet function. Nature Reviews Endocrinology 2022;18:9-22
2. Farnsworth NL, Hemmati A, Pozzoli M, Benninger RKP: Fluorescence recovery after photobleaching reveals regulation and distribution of connexin36 gap junction coupling within mouse islets of Langerhans. The Journal of Physiology 2014;592:4431-4446
3. Salomon D, Meda P: Heterogeneity and contact-dependent regulation of hormone secretion by individual B cells. Experimental Cell Research 1986;162:507-520
4. Katsuta H, Aguayo-Mazzucato C, Katsuta R, Akashi T, Hollister-Lock J, Sharma AJ, Bonner-Weir S, Weir GC: Subpopulations of GFP-Marked Mouse Pancreatic β-Cells Differ in Size, Granularity, and Insulin Secretion. Endocrinology 2012;153:5180-5187

5. Karaca M, Castel J, Tourrel-Cuzin C, Brun M, Géant A, Dubois M, Catesson S, Rodriguez M, Luquet S, Cattan P, Lockhart B, Lang J, Ktorza A, Magnan C, Kargar C: Exploring Functional β-Cell Heterogeneity In Vivo Using PSA-NCAM as a Specific Marker. PLOS ONE 2009;4:e5555
6. Kravets V, Dwulet JM, Schleicher WE, Hodson DJ, Davis AM, Pyle L, Piscopio RA, Sticco-Ivins M, Benninger RKP: Functional architecture of pancreatic islets identifies a population of first responder cells that drive the first-phase calcium response. PLoS Biol 2022;20:e3001761
7. Johnston Natalie R, Mitchell Ryan K, Haythorne E, Pessoa Maria P, Semplici F, Ferrer J, Piemonti L, Marchetti P, Bugliani M, Bosco D, Berishvili E, Duncanson P, Watkinson M, Broichhagen J, Trauner D, Rutter Guy A, Hodson David J: Beta Cell Hubs Dictate Pancreatic Islet Responses to Glucose. Cell Metabolism 2016;24:389-401
8. Salem V, Silva LD, Suba K, Georgiadou E, Neda Mousavy Gharavy S, Akhtar N, Martin-Alonso A, Gaboriau DCA, Rothery SM, Stylianides T, Carrat G, Pullen TJ, Singh SP, Hodson DJ, Leclerc I, Shapiro AMJ, Marchetti P, Briant LJB, Distaso W, Ninov N, Rutter GA: Leader β-cells coordinate Ca2+ dynamics across pancreatic islets in vivo. Nature Metabolism 2019;1:615-629
9. Bader E, Migliorini A, Gegg M, Moruzzi N, Gerdes J, Roscioni SS, Bakhti M, Brandl E, Irmler M, Beckers J, Aichler M, Feuchtinger A, Leitzinger C, Zischka H, Wang-Sattler R, Jastroch M, Tschöp M, Machicao F, Staiger H, Häring H-U, Chmelova H, Chouinard JA, Oskolkov N, Korsgren O, Speier S, Lickert H: Identification of proliferative and mature β-cells in the islets of Langerhans. Nature 2016;535:430-434
10. Benninger RKP, Hodson DJ: New Understanding of β-Cell Heterogeneity and In Situ Islet Function. Diabetes 2018;67:537-547
11. Caicedo A: Paracrine and autocrine interactions in the human islet: More than meets the eye. Seminars in Cell & Developmental Biology 2013;24:11-21
12. Huising MO, van der Meulen T, Huang JL, Pourhosseinzadeh MS, Noguchi GM: The Difference δ-Cells Make in Glucose Control. Physiology 2018;33:403-411
13. Moens K, Flamez D, Van Schravendijk C, Ling Z, Pipeleers D, Schuit F: Dual glucagon recognition by pancreatic beta-cells via glucagon and glucagon-like peptide 1 receptors. Diabetes 1998;47:66-72
14. Marchetti P, Lupi R, Bugliani M, Kirkpatrick CL, Sebastiani G, Grieco FA, Del Guerra S, D'Aleo V, Piro S, Marselli L, Boggi U, Filipponi F, Tinti L, Salvini L, Wollheim CB, Purrello F, Dotta F: A local glucagon-like peptide 1 (GLP-1) system in human pancreatic islets. Diabetologia 2012;55:3262-3272
15. Holter MM, Saikia M, Cummings BP: Alpha-cell paracrine signaling in the regulation of beta-cell insulin secretion. Frontiers in Endocrinology 2022;13
16. Hughes JW, Cho JH, Conway HE, DiGruccio MR, Ng XW, Roseman HF, Abreu D, Urano F, Piston DW: Primary cilia control glucose homeostasis via islet paracrine interactions. Proceedings of the National Academy of Sciences 2020;117:8912-8923
17. Hill TG, Hill DJ: The Importance of Intra-Islet Communication in the Function and Plasticity of the Islets of Langerhans during Health and Diabetes. In *International Journal of Molecular Sciences*, 2024
18. Balasenthilkumaran NV, Whitesell JC, Pyle L, Friedman RS, Kravets V: Network approach reveals preferential T-cell and macrophage association with α-linked β-cells in early stage of insulitis in NOD mice. Frontiers in Network Physiology 2024;4
19. Anquetil F, Sabouri S, Thivolet C, Rodriguez-Calvo T, Zapardiel-Gonzalo J, Amirian N, Schneider D, Castillo E, Lajevardi Y, von Herrath MG: Alpha cells, the main source of IL-1β in human pancreas. J Autoimmun 2017;81:68-73

20. Benkahla MA, Sabouri S, Kiosses WB, Rajendran S, Quesada-Masachs E, von Herrath MG: HLA class I hyper-expression unmasks beta cells but not alpha cells to the immune system in pre-diabetes. Journal of Autoimmunity 2021;119:102628
21. Nunemaker CS, Zhang M, Wasserman DH, McGuinness OP, Powers AC, Bertram R, Sherman A, Satin LS: Individual Mice Can Be Distinguished by the Period of Their Islet Calcium Oscillations : Is There an Intrinsic Islet Period That Is Imprinted In Vivo? Diabetes 2005;54:3517-3522
22. Nunemaker CS, Wasserman DH, McGuinness OP, Sweet IR, Teague JC, Satin LS: Insulin secretion in the conscious mouse is biphasic and pulsatile. Am J Physiol Endocrinol Metab 2006;290:E523-529
23. Curry DL, L. BL, Grodsky GM: Dynamics of Insulin Secretion by the Perfused Rat Pancreas. Endocrinology 1968;83:572-584
24. Porte D, Pupo AA: Insulin responses to glucose: evidence for a two pool system in man. J Clin Invest 1969;48:2309-2319
25. Benninger RKP, Zhang M, Head WS, Satin LS, Piston DW: Gap Junction Coupling and Calcium Waves in the Pancreatic Islet. Biophysical Journal 2008;95:5048-5061
26. Ravier MA, Güldenagel M, Charollais A, Gjinovci A, Caille De, Söhl G, Wollheim CB, Willecke K, Henquin J-C, Meda P: Loss of Connexin36 Channels Alters β-Cell Coupling, Islet Synchronization of Glucose-Induced Ca2+ and Insulin Oscillations, and Basal Insulin Release. Diabetes 2005;54:1798-1807
27. Zmazek J, Klemen MS, Markovič R, Dolenšek J, Marhl M, Stožer A, Gosak M: Assessing Different Temporal Scales of Calcium Dynamics in Networks of Beta Cell Populations. Frontiers in Physiology 2021;12
28. Stožer A, Gosak M, Dolenšek J, Perc M, Marhl M, Rupnik MS, Korošak D: Functional connectivity in islets of Langerhans from mouse pancreas tissue slices. PLoS Comput Biol 2013;9:e1002923
29. Stožer A, Dolenšek J, Rupnik MS: Glucose-Stimulated Calcium Dynamics in Islets of Langerhans in Acute Mouse Pancreas Tissue Slices. PLOS ONE 2013;8:e54638
30. Schindelin J, Arganda-Carreras I, Frise E, Kaynig V, Longair M, Pietzsch T, Preibisch S, Rueden C, Saalfeld S, Schmid B, Tinevez J-Y, White DJ, Hartenstein V, Eliceiri K, Tomancak P, Cardona A: Fiji: an open-source platform for biological-image analysis. Nature Methods 2012;9:676-682
31. Karlöf L, Ølgård TA, Godtliebsen F, Kaczmarska M, Fischer H: Statistical techniques to select detection thresholds for peak signals in ice-core data. Journal of Glaciology 2005;51:655-662
32. Šterk M, Dolenšek J, Skelin Klemen M, Križančić Bombek L, Paradiž Leitgeb E, Kerčmar J, Perc M, Slak Rupnik M, Stožer A, Gosak M: Functional characteristics of hub and wave-initiator cells in β cell networks. Biophys J 2023;122:784-801
33. Šterk M, Zhang Y, Pohorec V, Leitgeb EP, Dolenšek J, Benninger RKP, Stožer A, Kravets V, Gosak M: Network representation of multicellular activity in pancreatic islets: Technical considerations for functional connectivity analysis. PLOS Computational Biology 2024;20:e1012130
34. Zhang Q, Galvanovskis J, Abdulkader F, Partridge CJ, Göpel SO, Eliasson L, Rorsman P: Cell coupling in mouse pancreatic beta-cells measured in intact islets of Langerhans. Philos Trans A Math Phys Eng Sci 2008;366:3503-3523
35. Kravets V, Levitt CH, Benninger RK: 195-OR: To Which Degree Do Alpha Cells Shape the Role of the Beta Cells First Responders? Diabetes 2023;72
36. Duh M, Šterk M, Križančić Bombek L, MacDonald PE, Stožer A, Gosak M: Spatially bound functional heterogeneity drives modular organization in β-cell networks. Biophysical Journal 2025;124:3008-3022

37. Ren H, Li Y, Han C, Yu Y, Shi B, Peng X, Zhang T, Wu S, Yang X, Kim S, Chen L, Tang C: Pancreatic α and β cells are globally phase-locked. Nat Commun 2022;13:3721
38. Briggs JK, Gresch A, Marinelli I, Dwulet JM, Albers DJ, Kravets V, Benninger RKP: β-cell intrinsic dynamics rather than gap junction structure dictates subpopulations in the islet functional network. Elife 2023;12
39. Suba K, Patel Y, Martin-Alonso A, Hansen B, Xu X, Roberts A, Norton M, Chung P, Shrewsbury J, Kwok R, Kalogianni V, Chen S, Liu X, Kalyviotis K, Rutter GA, Jones B, Minnion J, Owen BM, Pantazis P, Distaso W, Drucker DJ, Tan TM, Bloom SR, Murphy KG, Salem V: Intra-islet glucagon signalling regulates beta-cell connectivity, first-phase insulin secretion and glucose homoeostasis. Mol Metab 2024;85:101947
40. Capozzi ME, Svendsen B, Encisco SE, Lewandowski SL, Martin MD, Lin H, Jaffe JL, Coch RW, Haldeman JM, MacDonald PE, Merrins MJ, D'Alessio DA, Campbell JE: β Cell tone is defined by proglucagon peptides through cAMP signaling. JCI Insight 2019;4
41. Svendsen B, Larsen O, Gabe MBN, Christiansen CB, Rosenkilde MM, Drucker DJ, Holst JJ: Insulin Secretion Depends on Intra-islet Glucagon Signaling. Cell Rep 2018;25:1127-1134.e1122
42. Capozzi ME, Wait JB, Koech J, Gordon AN, Coch RW, Svendsen B, Finan B, D'Alessio DA, Campbell JE: Glucagon lowers glycemia when β-cells are active. JCI Insight 2019;5
43. Tian G, Sandler S, Gylfe E, Tengholm A: Glucose- and hormone-induced cAMP oscillations in α- and β-cells within intact pancreatic islets. Diabetes 2011;60:1535-1543
44. Stožer A, Paradiž Leitgeb E, Pohorec V, Dolenšek J, Križančić Bombek L, Gosak M, Skelin Klemen M: The Role of cAMP in Beta Cell Stimulus-Secretion and Intercellular Coupling. Cells 2021;10
45. Wan QF, Dong Y, Yang H, Lou X, Ding J, Xu T: Protein kinase activation increases insulin secretion by sensitizing the secretory machinery to Ca2+. J Gen Physiol 2004;124:653-662
46. Kasai H, Hatakeyama H, Ohno M, Takahashi N: Exocytosis in islet beta-cells. Adv Exp Med Biol 2010;654:305-338
47. Light PE, Manning Fox JE, Riedel MJ, Wheeler MB: Glucagon-like peptide-1 inhibits pancreatic ATP-sensitive potassium channels via a protein kinase A- and ADP-dependent mechanism. Mol Endocrinol 2002;16:2135-2144
48. Lu M, Wheeler MB, Leng XH, Boyd AE, 3rd: The role of the free cytosolic calcium level in beta-cell signal transduction by gastric inhibitory polypeptide and glucagon-like peptide I(7-37). Endocrinology 1993;132:94-100
49. Holz GG, Leech CA, Heller RS, Castonguay M, Habener JF: cAMP-dependent mobilization of intracellular Ca2+ stores by activation of ryanodine receptors in pancreatic beta-cells. A Ca2+ signaling system stimulated by the insulinotropic hormone glucagon-like peptide-1-(7-37). J Biol Chem 1999;274:14147-14156
50. Islam MS: The ryanodine receptor calcium channel of beta-cells: molecular regulation and physiological significance. Diabetes 2002;51:1299-1309
51. Kim BJ, Park KH, Yim CY, Takasawa S, Okamoto H, Im MJ, Kim UH: Generation of nicotinic acid adenine dinucleotide phosphate and cyclic ADP-ribose by glucagon-like peptide-1 evokes Ca2+ signal that is essential for insulin secretion in mouse pancreatic islets. Diabetes 2008;57:868-878
52. Kang G, Chepurny OG, Rindler MJ, Collis L, Chepurny Z, Li WH, Harbeck M, Roe MW, Holz GG: A cAMP and Ca2+ coincidence detector in support of Ca2+-induced Ca2+ release in mouse pancreatic beta cells. J Physiol 2005;566:173-188
53. Paradiž Leitgeb E, Kerčmar J, Križančić Bombek L, Pohorec V, Skelin Klemen M, Slak Rupnik M, Gosak M, Dolenšek J, Stožer A: Exendin-4 affects calcium signalling

predominantly during activation and activity of beta cell networks in acute mouse pancreas tissue slices. Frontiers in Endocrinology 2024;Volume 14 - 2023
54. Shuai H, Xu Y, Ahooghalandari P, Tengholm A: Glucose-induced cAMP elevation in β-cells involves amplification of constitutive and glucagon-activated GLP-1 receptor signalling. Acta Physiol (Oxf) 2021;231:e13611
55. Aslanidi OV, Mornev OA, Skyggebjerg O, Arkhammar P, Thastrup O, Sørensen MP, Christiansen PL, Conradsen K, Scott AC: Excitation wave propagation as a possible mechanism for signal transmission in pancreatic islets of Langerhans. Biophys J 2001;80:1195-1209
56. Baltrusch S, Lenzen S: Regulation of [Ca2+]i oscillations in mouse pancreatic islets by adrenergic agonists. Biochem Biophys Res Commun 2007;363:1038-1043
57. Cane MC, Parrington J, Rorsman P, Galione A, Rutter GA: The two pore channel TPC2 is dispensable in pancreatic β-cells for normal Ca^{2+} dynamics and insulin secretion. Cell Calcium 2016;59:32-40
58. Zaborska KE, Jordan KL, Thorson AS, Dadi PK, Schaub CM, Nakhe AY, Dickerson MT, Lynch JC, Weiss AJ, Dobson JR, Jacobson DA: Liraglutide increases islet Ca. Diabetes Obes Metab 2022;24:1741-1752
59. Tengholm A, Gylfe E: cAMP signalling in insulin and glucagon secretion. Diabetes Obes Metab 2017;19 Suppl 1:42-53
60. Delgadillo-Silva LF, Tasöz E, Singh SP, Chawla P, Georgiadou E, Gompf A, Rutter GA, Ninov N: Optogenetic β cell interrogation in vivo reveals a functional hierarchy directing the Ca. Sci Adv 2024;10:eado4513
61. Peng X, Ren H, Yang L, Tong S, Zhou R, Long H, Wu Y, Wang L, Wu Y, Zhang Y, Shen J, Zhang J, Qiu G, Wang J, Han C, Zhang Y, Zhou M, Zhao Y, Xu T, Tang C, Chen Z, Liu H, Chen L: Readily releasable β cells with tight Ca2+–exocytosis coupling dictate biphasic glucose-stimulated insulin secretion. Nature Metabolism 2024;6:238-253
62. Zhang F, Zhang L, Qi Y, Xu H: Mitochondrial cAMP signaling. Cell Mol Life Sci 2016;73:4577-4590

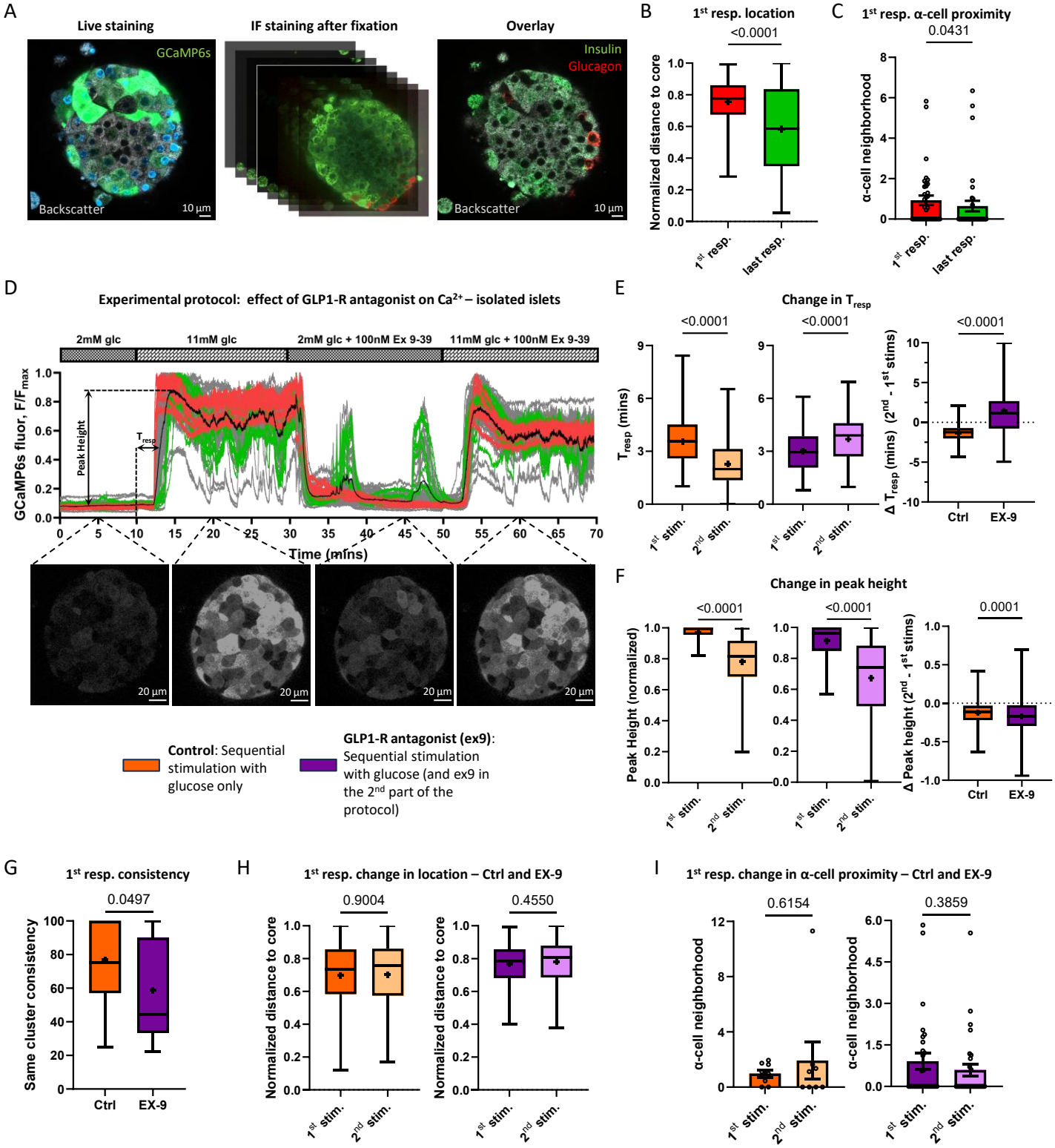
A
Live staining
IF staining after fixation
Overlay
GCaMP6s
Backscatter
10 µm
Insulin
Glucagon
B
1st resp. location
<0.0001
Normalized distance to core
1st resp.
last resp.
C
1st resp. α-cell proximity
0.0431
α-cell neighborhood
D
Experimental protocol: effect of GLP1-R antagonist on Ca2+ – isolated islets
2mM glc
11mM glc
2mM glc + 100nM Ex 9-39
11mM glc + 100nM Ex 9-39
GCaMP6s fluor, F/Fmax
Peak Height
Tresp
Time (mins)
20 µm
Control: Sequential stimulation with glucose only
GLP1-R antagonist (ex9): Sequential stimulation with glucose (and ex9 in the 2nd part of the protocol)
E
Change in Tresp
Tresp (mins)
Δ Tresp (mins) (2nd - 1st stims)
1st stim.
2nd stim.
Ctrl
EX-9
F
Change in peak height
Peak Height (normalized)
Δ Peak height (2nd - 1st stims)
0.0001
G
1st resp. consistency
0.0497
Same cluster consistency
H
1st resp. change in location – Ctrl and EX-9
0.9004
0.4550
I
1st resp. change in α-cell proximity – Ctrl and EX-9
0.6154
0.3859

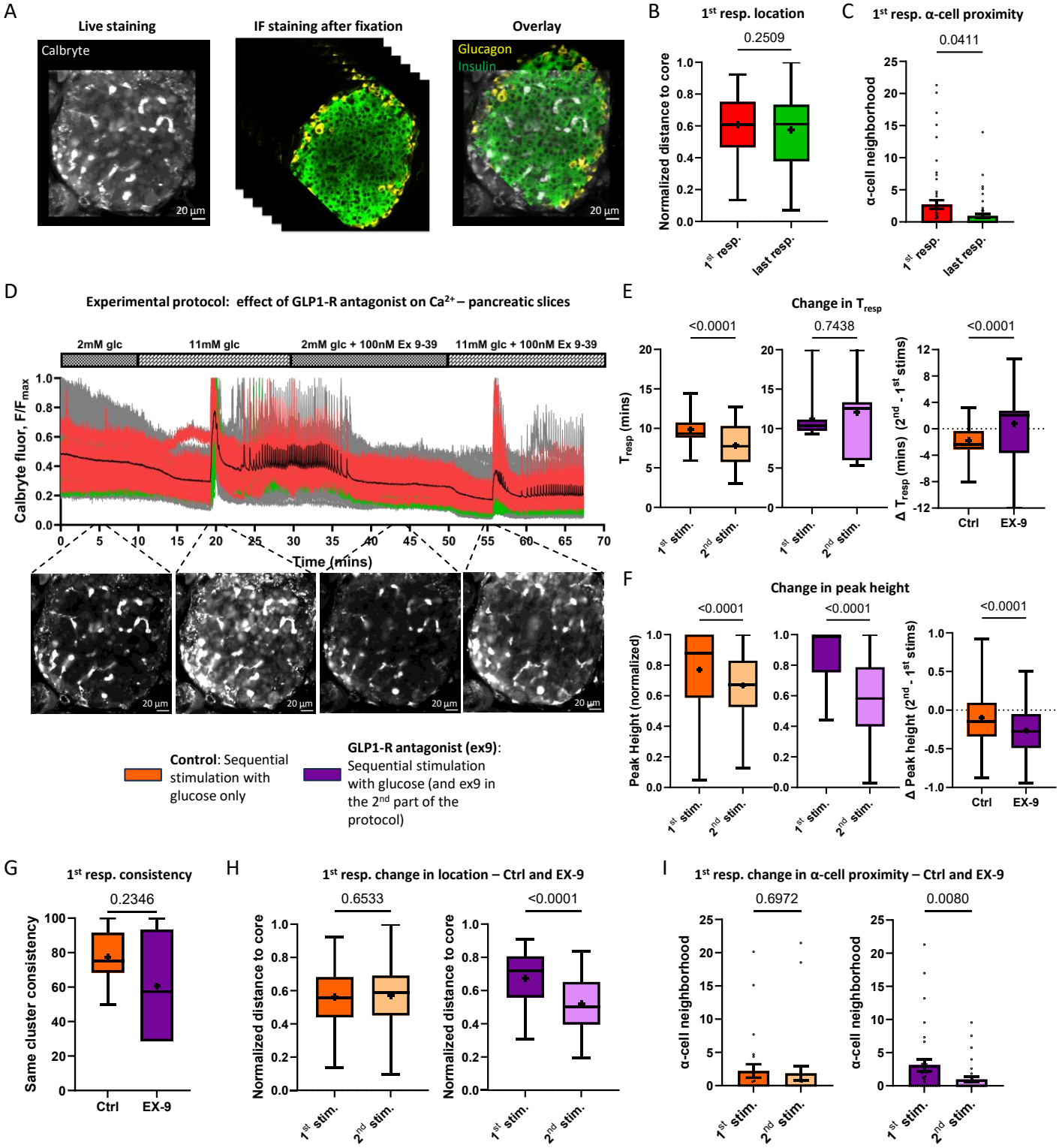
A
Live staining
Calbryte
20 µm
IF staining after fixation
Overlay
Glucagon
Insulin
20 µm
B
1st resp. location
0.2509
Normalized distance to core
1st resp.
last resp.
C
1st resp. α-cell proximity
0.0411
α-cell neighborhood
1st resp.
last resp.
D
Experimental protocol: effect of GLP1-R antagonist on Ca2+ – pancreatic slices
2mM glc
11mM glc
2mM glc + 100nM Ex 9-39
11mM glc + 100nM Ex 9-39
Calbryte fluor, F/Fmax
Time (mins)
20 µm
Control: Sequential stimulation with glucose only
GLP1-R antagonist (ex9): Sequential stimulation with glucose (and ex9 in the 2nd part of the protocol)
E
Change in Tresp
<0.0001
0.7438
<0.0001
Tresp (mins)
Δ Tresp (mins) (2nd - 1st stims)
1st stim.
2nd stim.
Ctrl
EX-9
F
Change in peak height
<0.0001
<0.0001
<0.0001
Peak Height (normalized)
Δ Peak height (2nd - 1st stims)
1st stim.
2nd stim.
Ctrl
EX-9
G
1st resp. consistency
0.2346
Same cluster consistency
Ctrl
EX-9
H
1st resp. change in location – Ctrl and EX-9
0.6533
<0.0001
Normalized distance to core
1st stim.
2nd stim.
I
1st resp. change in α-cell proximity – Ctrl and EX-9
0.6972
0.0080
α-cell neighborhood
1st stim.
2nd stim.

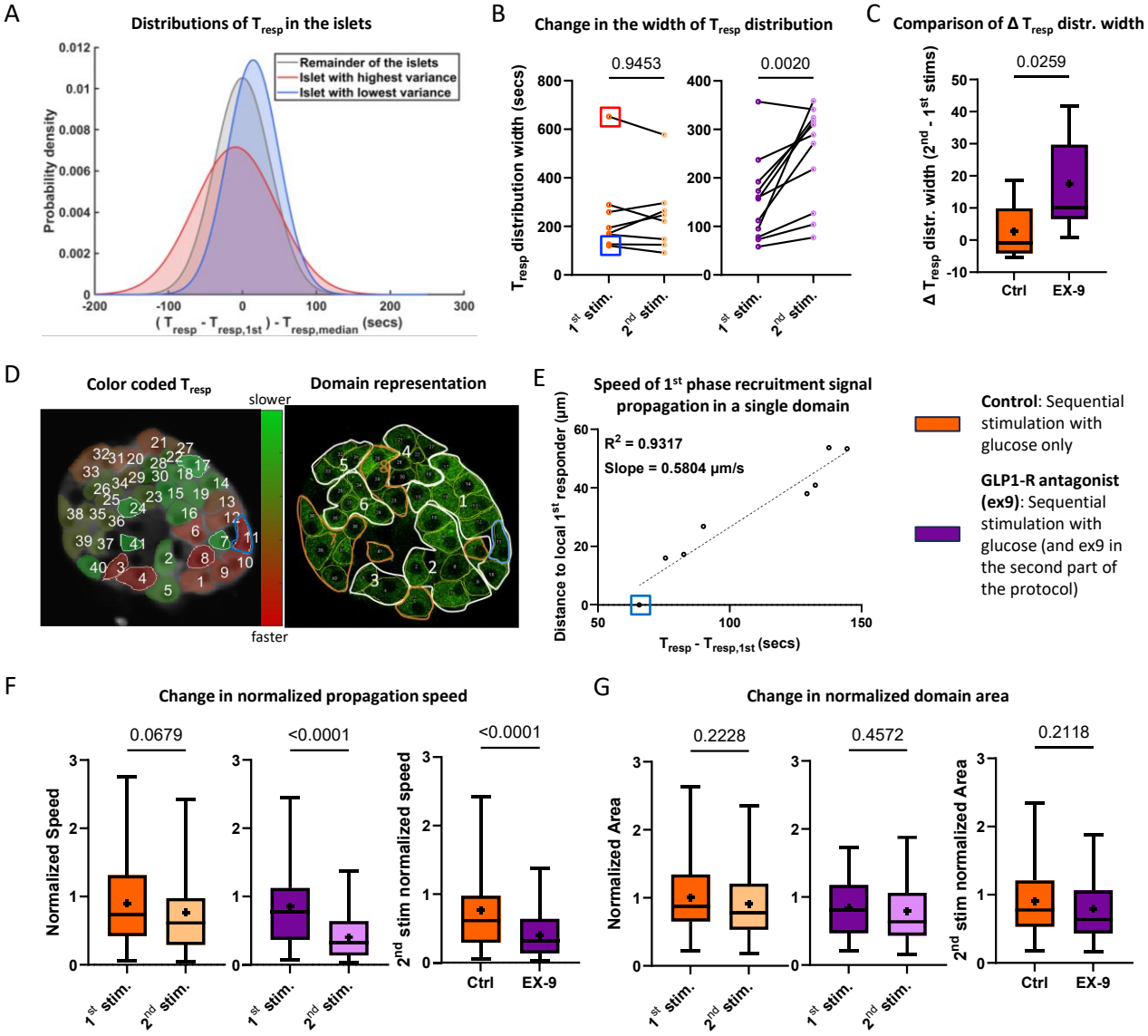
A
Distributions of T_{resp} in the islets
Remainder of the islets
Islet with highest variance
Islet with lowest variance
Probability density
$(T_{resp} - T_{resp,1st}) - T_{resp,median}$ (secs)
B
Change in the width of T_{resp} distribution
T_{resp} distribution width (secs)
0.9453
0.0020
1st stim.
2nd stim.
C
Comparison of Δ T_{resp} distr. width
Δ T_{resp} distr. width (2nd - 1st stims)
0.0259
Ctrl
EX-9
D
Color coded T_{resp}
Domain representation
slower
faster
E
Speed of 1st phase recruitment signal propagation in a single domain
R^2 = 0.9317
Slope = 0.5804 μm/s
Distance to local 1st responder (μm)
$T_{resp} - T_{resp,1st}$ (secs)
Control: Sequential stimulation with glucose only
GLP1-R antagonist (ex9): Sequential stimulation with glucose (and ex9 in the second part of the protocol)
F
Change in normalized propagation speed
Normalized Speed
0.0679
<0.0001
2nd stim normalized speed
<0.0001
1st stim.
2nd stim.
Ctrl
EX-9
G
Change in normalized domain area
Normalized Area
0.2228
0.4572
2nd stim normalized Area
0.2118
1st stim.
2nd stim.
Ctrl
EX-9

A

α- and δ-cell representation in the islet

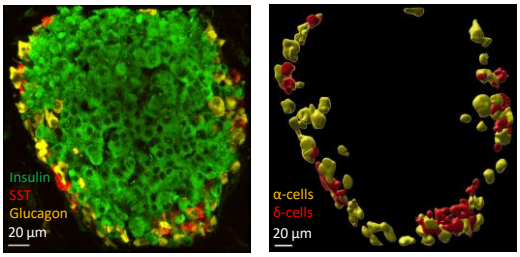

B

α-cell count vs frequency

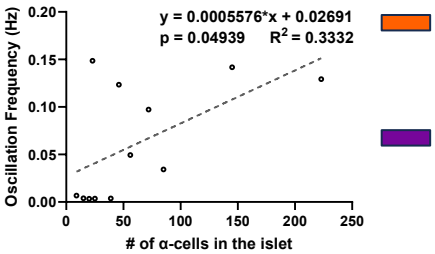

Control: Sequential stimulation with glucose only

GLP1-R antagonist (ex9): Sequential stimulation with glucose (and ex9 in the second part of the protocol)

C

Window selection for 2nd phase analysis

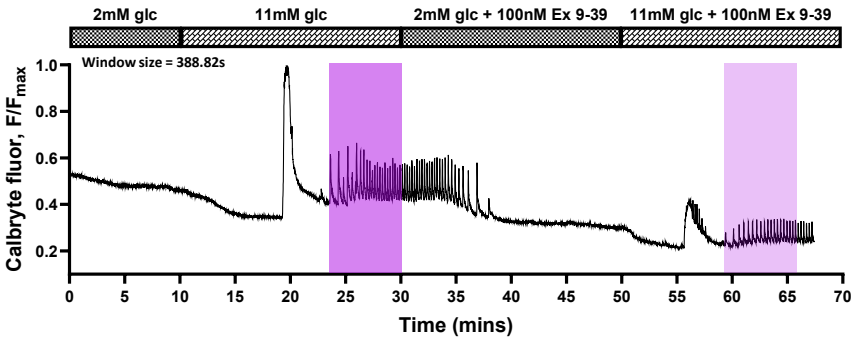

D

Change in frequency

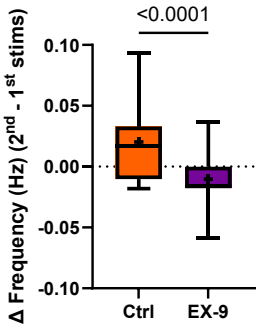

E

Distributions of frequency in the islets

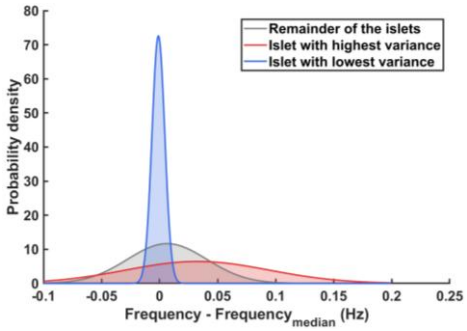

F

Change in frequency distribution – Ctrl and EX-9

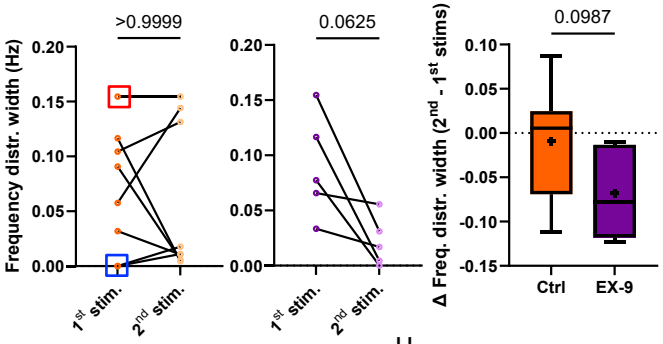

G

Representative images of slices (Control)

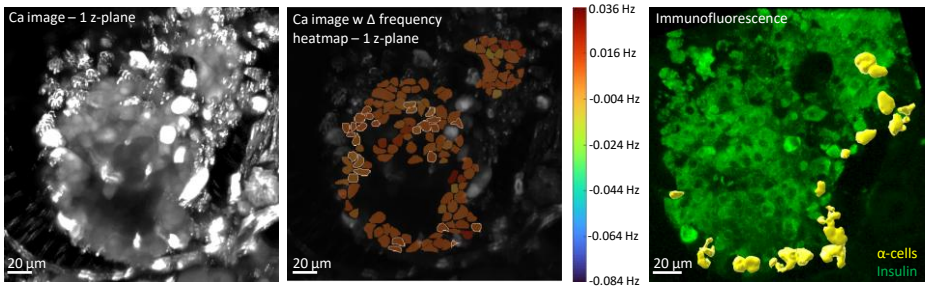

H

Δ Freq. w/ or w/o α- neighbors

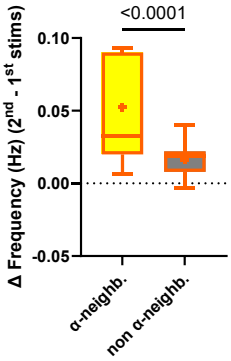

I

Representative images of slices (EX-9 treated)

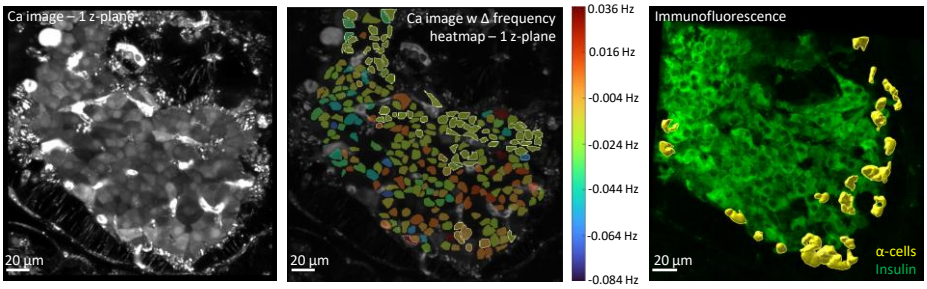

J

Δ Freq. w/ or w/o α- neighbors

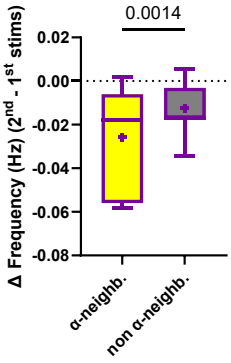

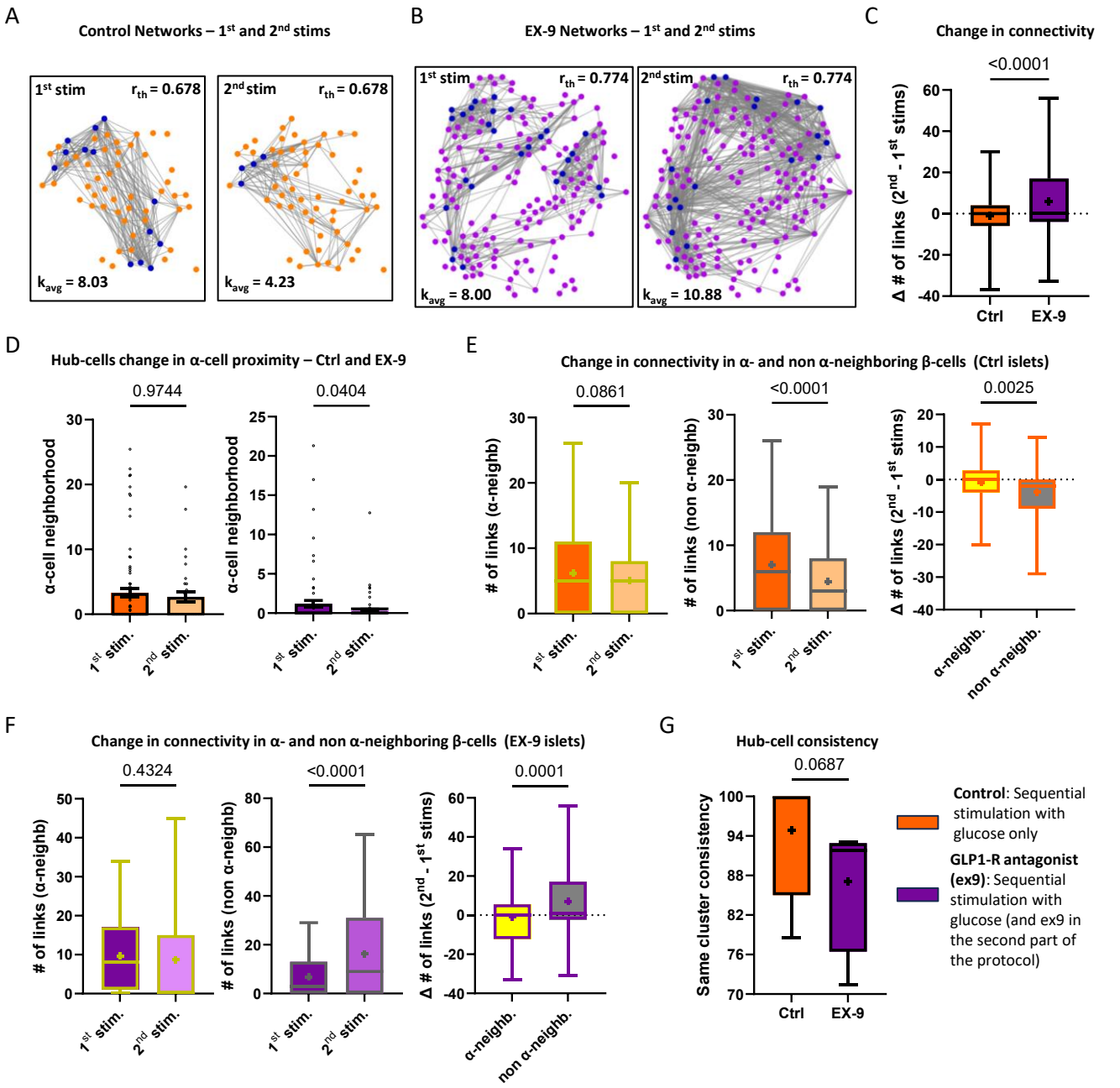
A
Control Networks – 1st and 2nd stims
1st stim
rth = 0.678
kavg = 8.03
2nd stim
rth = 0.678
kavg = 4.23
B
EX-9 Networks – 1st and 2nd stims
1st stim
rth = 0.774
kavg = 8.00
2nd stim
rth = 0.774
kavg = 10.88
C
Change in connectivity
<0.0001
Δ # of links (2nd - 1st stims)
Ctrl
EX-9
D
Hub-cells change in α-cell proximity – Ctrl and EX-9
0.9744
0.0404
α-cell neighborhood
1st stim.
2nd stim.
E
Change in connectivity in α- and non α-neighboring β-cells (Ctrl islets)
0.0861
<0.0001
0.0025
# of links (α-neighb)
# of links (non α-neighb)
Δ # of links (2nd - 1st stims)
α-neighb.
non α-neighb.
F
Change in connectivity in α- and non α-neighboring β-cells (EX-9 islets)
0.4324
<0.0001
0.0001
G
Hub-cell consistency
0.0687
Same cluster consistency
Control: Sequential stimulation with glucose only
GLP1-R antagonist (ex9): Sequential stimulation with glucose (and ex9 in the second part of the protocol)